Supplementary Material for:

Human endogenous retrovirus-K induces motor neuron disease

Wenxue Li, Myoung-Hwa Lee, Lisa Henderson, Richa Tyagi, Muzna Bachani, Joseph Steiner, Emilie Campanac, Dax Hoffman, Gloria von Geldern, Kory Johnson, Dragan Maric, H. Douglas Morris, Margaret Lentz, Katherine Pak, Andrew Mammen, Lyle Ostrow, Jeffrey Rothstein, Avindra Nath*

*Correspondence author. E-mail: natha@ninds.nih.gov

The PDF file includes:

Table S1. Clinical data for the human brain samples

Table S2. Passive and active membrane properties of mPFC L5 pyramidal neurons.

Table S3. Primer sequences

Movie S1. Hind limb clasping in a tail suspension test.

Supplementary Materials

Supplementary Materials and Methods

Magnetic resonance imaging: 9 months old wt (n = 5) and tg (n = 5) mice were subjected to MR imaging. Mice were perfused and fixed with 4% paraformaldehyde containing 0.5% Magnevist. The brains were then extracted and incubated in a same solution overnight for a post fixation. MR imaging was carried out in the NIH Mouse Image Facility. MR images were acquired on a 14 Tesla Bruker Biospec NMR spectrometer with microimaging gradients (Bruker Biospec, Inc, Billerica MA, USA) using a 3D FLASH sequence with the following parameter values; TE 3.9 ms, TR 50 ms, average number 1, Field-of-View of 22 x 14 x 11 mm and an acquisition matrix 512 × 325 × 256[40]. The image resolution is 43 microns isotropic over the entire brain. The MRI scans were stored into a Digital Images and Communications in Medicine (DICOM) image files and transferred to Medical Image Processing, Analysis and Visualization (MIPAV) software, where manual volumetric analysis was carried out. MIPAV allows the user to manually outline regions of interest (ROIs) and afterwards calculates the volumes of a specific ROI.

This study focused on measures of six brain regions: whole brain volume, motor cortex thickness and volume, cingulate cortex volume, corpus callosum thickness and hippocampus volume. ROIs were traced without reference to the genotype of the mice. Brain volumes were

calculated by multiplying the thickness of the slice (0.04 mm) by the area of the cross-section. The total volume for the region was calculated by summing these slice volumes. The perimeter of the entire rostral–caudal length of the brain was traced to calculate whole brain volume (Supplementary Fig. 7a). This included everything from the slice most similar to that labeled as Bregma +4.28 mm in a mouse brain atlas[41] to the slice most similar to that labeled Bregma -8.24 mm. The starting point was the beginning of the olfactory bulb, and the endpoint was the transition from the brainstem to the spinal cord. The motor cortex of mouse brain starts to appear at around Bregma +2.30 mm and ends at around Bregma -1.30 mm. The distance between brain surface and the top of the cingulum was measured (Supplementary Fig. 7b). Total nine brain slices between Bregma +1.09 mm and Bregma -0.51 mm were chosen to measure. The width of the cortex on both sides was averaged for each mouse. For volumetric analysis, the motor cortex was traced as they appeared on sagittal sections of the brain between those labeled as Bregma +1.09 mm and Bregma +0.25 mm (Supplementary Fig. 7c). The cingulate *cortex* was outlined by starting at the intersection of the corpus callosum with the midline and following the corpus callosum and cingulum to its most dorsolateral point. This point was then connected with a line to the most dorsal and medial intra-hemispheric point of the cortex (Supplementary Fig. 7d). Using this landmark-based method, the cingulate cortex was measured on nine slices starting rostrally at the closure of the genu of the corpus callosum (approximately Bregma +1.09 mm from Bregma) and terminating caudally at the rostral limit of the hippocampus (approximately -0.51 mm from Bregma). A line between its most dorsal point and its most ventral point at the intersection of the corpus callosum with the midline was drawn and measured to determine the corpus callosum thickness (Supplementary Fig. 7e). Nine cross-sections of MRI scans were measured between those labeled as Bregma +1.09 mm and Bregma -0.51 mm. The hippocampus

*(*cornu ammonis, CA) and dentate gyrus (DG) were manually outlined on cross-sections at the levels, approximately Bregma -1.55 mm, -1.91 mm and -2.27 mm (Supplementary Fig. 7f).

Behavioral analysis: Both male and female mice at 3 to 9 months of age were used. Mouse behavior was tracked using a video tracking software ANYmaze™ (Stoelting Co., Wood Dale, IL). Animals were returned to their cage during the inter-trial intervals and after the completion of each paradigm. All behavioral tests were conducted between 10 a.m. and 3 p.m. by an investigator blinded to the condition of the animal. However due to the prominent phenotypic changes in the tg animals such blinding was not successful in the older animals. Values of all behavioral analyses are presented as mean ± SEM. Sample sizes for animal used for each test are provided in the legend for Fig 5. Data was analyzed by Student's *t* test). All behavioral tests were conducted in a blinded manner. However due to the prominent phenotypic changes in the tg animals, such blinding was not successful in the older animals for motor tasks.

Open field task The open-field test was used to evaluate general locomotor activity, novel environment exploration and anxiety-like behavior in wt and tg mice. The open field was carried out in a square chamber of 40 cm^2 surface area and 35 cm high walls. It was divided equally into 16 squares by infrared photocell beams. The central 4 grids were considered to be the center, and the rest were assigned as the periphery. An automated system recorded each beam break as one unit of exploratory activity, similar to manual scoring of each line crossed. Mice were placed into a corner of the arena and were then allowed to freely explore the arena for 5 min. Their movement broke laser beams, and the tracking system automatically recorded each beam break as one unit of activity. During the observed time period, the number of grid lines crossed, vertical movements, latency to enter the center, time spent in the center and number of times the animal entered the center were recorded.

Tail suspension test Motor dysfunction was also assessed by monitoring clasping of the limbs, triggered by a tail suspension test[42]. The clasping score was assessed as previously described[42,43]. Mice at 6 months of age were suspended by the tails for 15 sec and the movements of hind limbs were observed. Mice were assessed by a clasping score. The score was rated 0 if no clasping was observed during a period of 15 sec, 1 if abnormal extension of the hind limbs was noticed, 2 if mouse started to clasp, and 3 if clasping it was firmly established.

Y-maze task: The Y-maze test assessed working memory by monitoring spontaneous alternation behavior in a Y-shaped maze. The apparatus was made of 3 acrylic plastic arms (35 cm length, 5 cm width, and 10 cm height) at 120 degrees to each other. Mice were placed in the center of the maze and were allowed to freely explore the three arms for 8 min. The maze activity was recorded via camera-based tracking system (Stoelting). To measure spontaneous alternation, the number of arm entries and the number of alternations were scored. Arm entry was defined as entry of all four paws of the mouse within the arm. Consecutive entries into three different arms were defined as alternations. Alternation percentage was calculated by dividing the number of alternations by the number of possible alternations and then multiplying by 100.

Sticky paper test: This somatosensory test was performed as previously described[44]. The animals were acclimated to the testing box (30×45 cm) for 1 min. Self-adhesive tape strips (0.3×0.4 cm) were placed onto the ventral side of the hind paw of mice. Animals were then replaced in the testing box and the performance on the task was video recorded and analyzed off-line. The latency of the first reaction to the stimulus (paw lifting, sniffing, biting, or removal) was measured.

Negative geotaxis test: Mice were placed on the inclined platform of 45 degree facing in a downward direction. The latency to turn and orient head-up from downhill initial position was

video-recorded. Delays in the ability to reorient are indicative of delays in vestibular dysfunction[45].

***In utero* electroporation:** Timed-pregnant female CD-1 mice from Charles River at embryonic day 14 were anesthetized with ketamine/xylazine (100/10 mixture; 0.1 mg/g body weight, i.p.). The uterine horns were exposed. A lateral ventricle of each embryo was injected with a mixture of plasmid DNA encoding HERV-K *env* (2 µg/µl) and tdTomato expression vector (1 µg/µl) with a glass micropipette made from a microcapillary tube (Sutter Instrument Co., Novato, CA, USA). Injected plasmid solution contained Fast Green solution (0.001%) to monitor the injection. The embryo's head in the uterus was held between the tweezers-type electrode, consisting of two disc electrodes of 5 mm diameter (CUY650-5, Nepa Gene Co., Chiba, Japan). The positive electrode was placed on the dorsal lateral side of the brain to target the cerebral cortex. According to the manufacturer's protocol, electrode pulses (35V, 50 ms) were charged 4 times at intervals of 950 ms with an electroporator (CUY21SC, Nepa Gene Co., Ichikawa-City, Japan). The uterine horn was placed back into the abdominal cavity and the abdominal wall and skin was sutured. At postnatal day14 the brains were removed, fixed and sectioned for imaging in mice electroporated with *env* DNA or a control DNA constructs. All images were obtained using a LSM 510 META laser-scanning confocal microscope (Carl Zeiss).

Electrophysiology: Six weeks old wt and tg mice were decapitated under isoflurane anesthesia and the brain was immediately excised and immersed in ice-cold solution containing (in mM): 90 sucrose, 80 NaCl, 1.3 KCl, 1 NaH_2PO_4, 25 NaHCO3, 2 $CaCl_2$, 1 $MgCl_2$, 10 mM glucose, 3 mM pyruvic acid; pH 7.2-7.3; 310 mOsm/l). Coronal slices (300 µm) containing the mPFC were cut with a vibrotome (Leica VT1200S). After recovery, incubation for ~ 15 min at 33°C was

followed by ~ 45 min at 22°C in artificial cerebrospinal fluid (ACSF; in mM: 125 NaCl, 2.5 KCl, 1 NaH_2PO_4, 25 $NaHCO_3$, 2 $CaCl_2$, 1 $MgCl_2$, 20 glucose, 3 mM Pyruvic acid; pH 7.2-7.3; 310 mOsm/l). Slices were then transferred to the recording chamber and superfused (2-3 ml min-1) with ACSF at 32-33°C. All solutions were saturated with 95% O_2, 5% CO_2. Whole-cell patch recordings were obtained from pyramidal neurons in layer 5 of the medial prefrontal cortex. The animals were coded so that electrophysiological experiments and analyses were performed blind with respect to genotype.

Current clamp To measure intrinsic properties (input resistance and excitability) currents steps (1s, -160 to +220 pA/20 pA step) were injected and all cells which were maintained at -65mV after membrane break-in and measurement of the resting membrane potential. Recordings were performed in the presence of 20 µM NBQX and 50 µM picrotoxin in the bath to block glutamatergic and GABAergic transmission, respectively and recording pipettes were filled with an internal solution containing (in mM): 125 K-gluconate, 20 KCl, 10 Hepes, 4 NaCl, 0.5 EGTA, 4 Mg ATP, 0.3 GTP, 10 phosphocreatine (pH 7.2, 290 mOsm).

Voltage clamp Spontaneous excitatory synaptic activity was recorded near the reversal potential of inhibition (-60mV) or of excitation (0mV) and patch electrodes were filled with (in mM): 125 K-gluconate, 4 KCl, 4 NaCl, 10 Hepes, 0.5 EGTA, 4 Mg ATP, 0.3 GTP, 10 phosphocreatine (pH 7.2, 290 mOsm).

Drugs All chemicals were purchased from Tocris (Ballwin, MO), Abcam (Cambridge, MA) or Sigma Chemical (St. Louis, MO).

Data acquisition and analysis Electrophysiological recordings were obtained using a multiclamp 700B amplifier and PClamp 10 (Molecular, Devices, Sunnyvale, CA). Data were analyzed using

Microsoft Excel, Minianalysis (Synaptosoft, Decatur, GA), and/or IGOR Pro (WaveMetrics, Lake Oswego, OR). Pooled data are presented as either mean ± SEM or box plots.

Product enhanced reverse transcriptase (PERT) assay: PERT assay was performed as previously published with minor modifications[46]. Briefly, cell supernatants were collected and centrifuged to pellet any cell debris. The cleared supernatant was then supplemented with 0.25% Triton X-100, 5 mM DTT and 0.25 mM EDTA to release HERV-K reverse transcriptase (RT). Bacteriophage MS2 genomic RNA was used as template for the reverse transcription reaction. For quantitative PCR, the following TaqMan primers and probe were used: forward primer 5'-TCCTGCTCAACTTCCTGTCGA-3', reverse primer 5'-CACAGGTCAAACCTCCTAGGAATG-3', and probe 5'-[6FAM]CGAGACGCTACCATGGCTATCGCTGTAG[TAM]-3'. Reverse transcriptase activity was expressed as fold change compared to control or as pg/ml RT determined by standard curve generated from PERT using HIV-1 RT.

Luciferase assay: All cell lines were obtained from ATCC and were tested for mycoplasma contamination prior to use. HeLa cells were seeded into 24-well plates 24 hours before transfection. Cells were transfected with pMetLuc-HEVRV-K-LTR and pcDNA3.1-TDP43 or other plasmids as indicated. 48 hr later, supernatants were collected and assayed for luciferase activity according to manufacturer's instruction (Clontech, Mountain View, CA). Relative luciferase activity was expressed as % relative luciferase units (RLU) for fold change relative to control.

Transfection of cells: Transfections were performed using Lipofectamine 2000 reagent according manufacturer's instructions (Life Technologies, Grand Island, NY). For knockdown

experiments, 50 nM ON-TARGET*plus* SMARTpool siRNA specific for TDP-43 (Thermo Scientific, Rockville MD) (Supplementary Fig. 10e) was transfected into cells using Lipofectamine siRNAmax (Life Technologies). Cells were harvested at 48 hr post-transfection, total RNA was extracted and HERV-K *gag* or *pol* transcripts were analyzed by RT-PCR. Neuronal cells were nucleofected with pcDNA control plasmid, HERV-K whole genome expression plasmid or TDP-43 construct using program DN-100 on the 4D-Nucleofector system (Lonza). Transcripts were expressed relative to □-actin or GAPDH endogenous control, as indicated in figure legends. Data represent at least three independent experiments. Values are shown as mean ± SEM and analyzed by Student's *t* test.

Biotin-streptavidin DNA-protein immunoprecipitation assay: Nuclear extracts (NE) from 293T cells were isolated using the NE-PER nuclear and cytoplasmic extraction kit, according to the manufacturer's protocol (Thermo Scientific). NE (100 □g) were incubat biotinylated DNA probe (corresponding to putative TDP-43 binding sites) for 15 min at room temperature. Streptavidin-conjugated magnetic Dynabeads (Invitrogen) were added and the mixture was incubated for an additional 30 min with slow mixing. Beads were pre-incubated with 1.0% bovine serum albumin (BSA) in phosphate-buffered saline (PBS) for 45 min prior to their addition to block non-specific interactions. The beads were then washed three times under low-stringency (PBS, 137 mM NaCl) or high-stringency conditions (10 mM Tris, pH 7.5, 1 mM EDTA, 300 mM NaCl) and resuspended in SDS loading buffer for western blot analysis. Equal volumes were loaded and run on a 4-12% (w/v) Bis-Tris electrophoresis gel (Life Technologies). The proteins were then transferred onto a PVDF membrane and immunoblotted with an antibody against TDP-43 (Abcam). Optical density of the bands was measured and expressed relative to

that obtained from TDP-43 binding to nt726. Values represent mean ± SEM of three independent experiments.

Chromatin immunoprecipitation (ChIP) and quantitative real-time PCR: HeLa cells at approximately 50% confluence were transiently transfected with HERV-K 5'LTR-luciferase construct or pcDNA3.1(+) control vector with or without plasmid encoding wild-type TDP-43. 48 hr post-transfection, cells were fixed in fresh 1.0% (w/v) paraformaldehyde and ChIP was performed using the Epigentek Chromaflash One-Step ChIP Kit with antibodies against RNA Polymerase II (phosph-S2; Abcam) or TDP-43 (Abcam). An isotype IgG control antibody (Epigentek, Farmingdale, NY) was included in all experiments. Primers used to amplify HERV-K LTR were: forward 5'- GTTTGTCTGCTGACCCTCTC-3' and reverse 5'-CCTGTGGGTGTTTCTCGTAAG-3' to amplify a 231 bp region encompassing the transcription initiation site; forward 5'-GGAAAGCCAGGTATTGTCCA-3' and reverse 5'-CTCCTCAGCACAGACCCTTT-3' to amplify a 120 bp region that encompassed nt343; forward 5'-GGGCAGCAATACTGCTTTGT-3' and reverse 5'-TTCTCAAAGAGGGGGATGTG-3' to amplify a 174 bp region that encompassed nt726 and nt761; and forward 5'-CACATCCCCCTCTTTGAGAA-3' and reverse 5'-CTCGTAAGGTGGGACGAGAG-3' to amplify a 174 bp region that encompassed nt866 and nt893. Negative control reactions were also performed using primers for an unrelated sequence (GAPDH promoter): forward 5'-TACTAGCGGTTTTACGGGCG-3' and reverse 5'-TCGAACAGGAGGAGCAGAGAGCGA-3'. Real-time PCR was performed using the Fast SYBR Green Supermix kit (Life Technologies) in a ViiA 7 Real-Time PCR system (Applied Biosystems). Fold-change in binding was calculated by relative quantitation using the comparative threshold cycle (Ct) method, with

results reported relative to control IgG ($\Delta CT = CT_{Target} - CT_{IgG\ control}$; fold change relative to IgG control = $2^{-\Delta Ct}$). Values represent mean ± SEM of three independent experiments.

Supplementary Figures

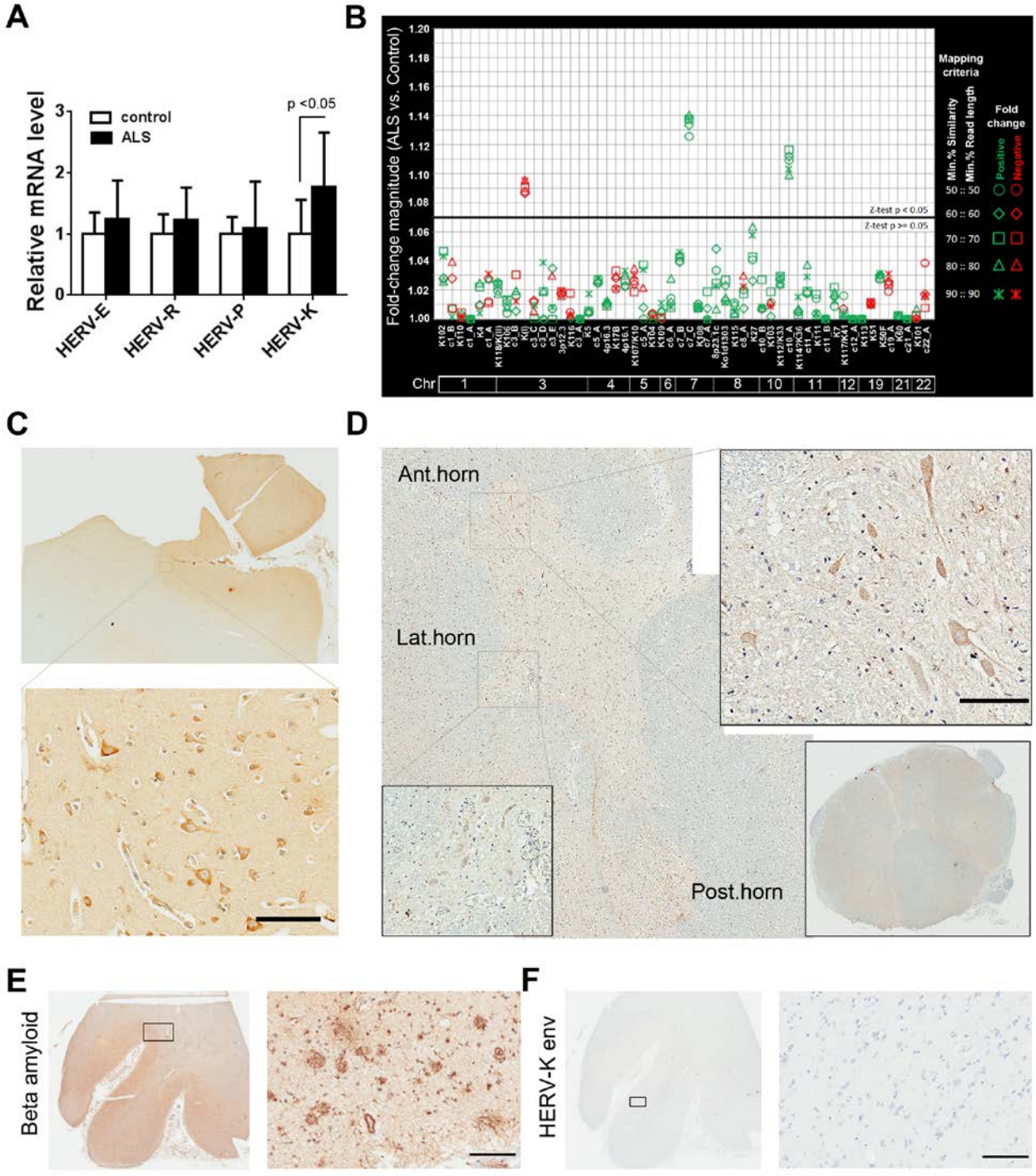

Fig. S1. HERV-K expression in autopsied human brain. (**A**) Expression of a panel of HERVs was determined autopsy brain tissue from frontal cortex of patients with ALS by RT-PCR and compared to controls. Only HERV-K transcript was significantly elevated in the ALS brain samples. (**B**) HERV-K expression between ALS and control by RNA-Seq was compared. Differential expression between three ALS subjects and three controls is explained in Fold-Change Magnitude units (y-axis) for 54 select genomic regions (x-axis). Genomic regions selected include those previously reported [1,2] to contain HERV-K sequence elements. Symbols depicted describe the Fold-Change Magnitude that results when different read-to-reference mapping criteria are used (i.e., Minimum % Similarity, Minimum % Read Length). Symbol color indicates whether the difference in mean expression for a genomic region between ALS and control was positive (green) or negative (red). Of the 54 genomic regions represented, three regions have a mean difference in expression between ALS and control that is significantly larger than those observed for all other regions (Z-test, $p < 0.05$). Specifically, regions c7_C and c10_A have significantly larger positive mean differences than any other region while region K(I) has a significantly larger negative mean differences than any other region. When mean differences in expression between ALS and control are tested by region via Welch-modified t-test or expression is tested accumulatively across all regions, none provide a corrected $p < 0.05$. (**C**) Human autopsied frontal cortex and (**D**) the spinal cord from patients with ALS were immunostained with anti-HERV-K env antibody. (**E**) Autopsied frontal cortex of a Alzheimer's patient was immunoreactive with anti-beta amyloid but not with (**F**) anti-HERV-K env antibody.. Scale bars are 100 µm (**C**, **D**) and 20 µm (**E**,**F**).

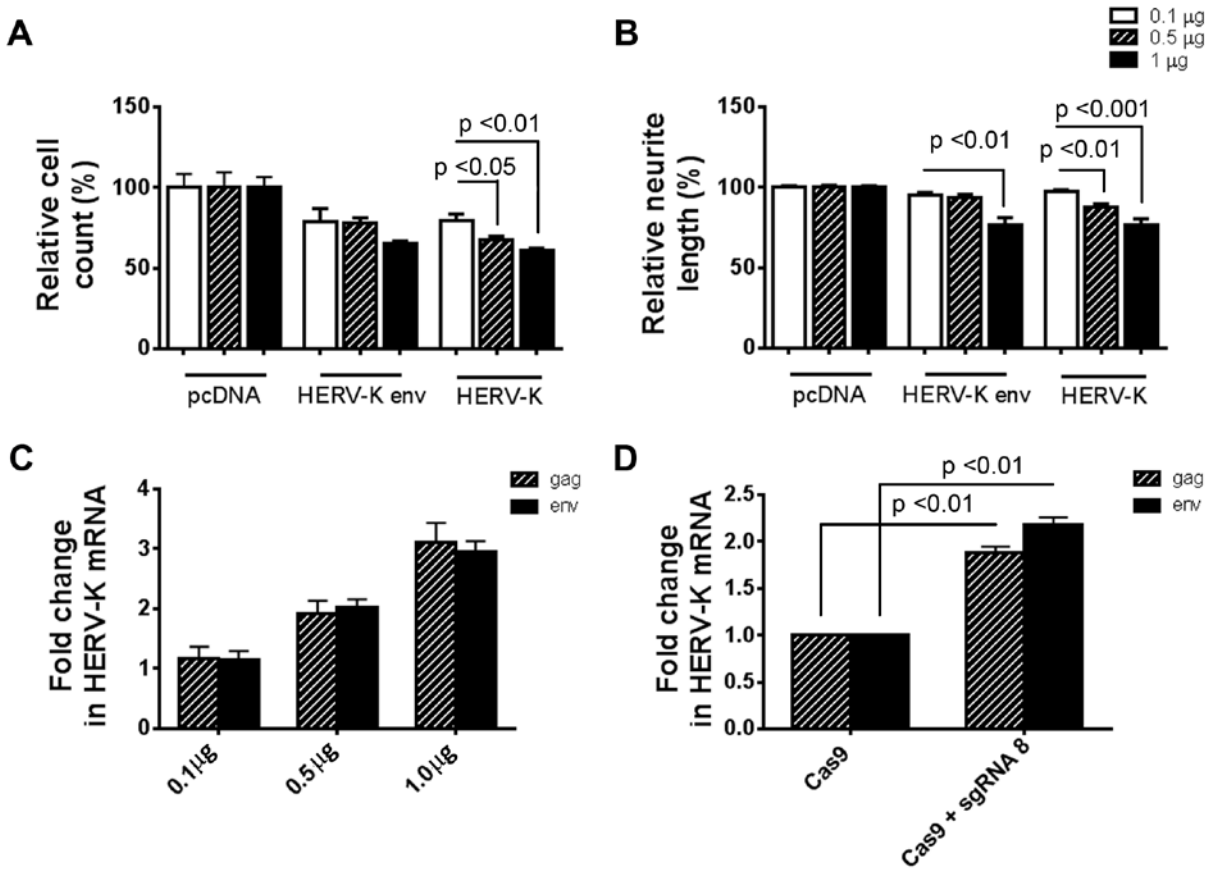

Fig. S2. Induction of HERV-K expression in human neurons. (**A,B**) Plasmids with either HERV-K *env* or complete HERV-K genome were transfected into pluripotent stem cell-derived human neurons expressing td-Tomato and monitored for morphological changes. pcDNA were used as a control. At 24 hours post transfection, the neurons transfected with HERV-K *env* and HERV-K showed decreases in (**A**) cell numbers and (**B**) neurite length in a dose-dependent manner. All experiments were performed in replicates of 18 and repeated twice. (**C**) Neural stem cell (NSC)-derived neurons were transfected with pcDNA control or increasing amounts of HERV-K expression construct as indicated. 24 hours post-transfection, cells were collected for RNA extraction and qRT-PCR to detect HERV-K transcripts. (**D**) NSC-derived neurons were transduced with a lentiviral construct encoding Cas9 fused to transcription activation domain VP64 for 24 hours. Cells were either treated with Cas9 alone or transduced with guide RNA

targeting the HERV-K promoter (sgRNA 8). 24 hours after sgRNA treatment, cells were collected for RNA extraction and qRT-PCR to detect HERV-K transcripts. Values represent mean ± SEM from three independent experiments and were analyzed by Student's *t* test.

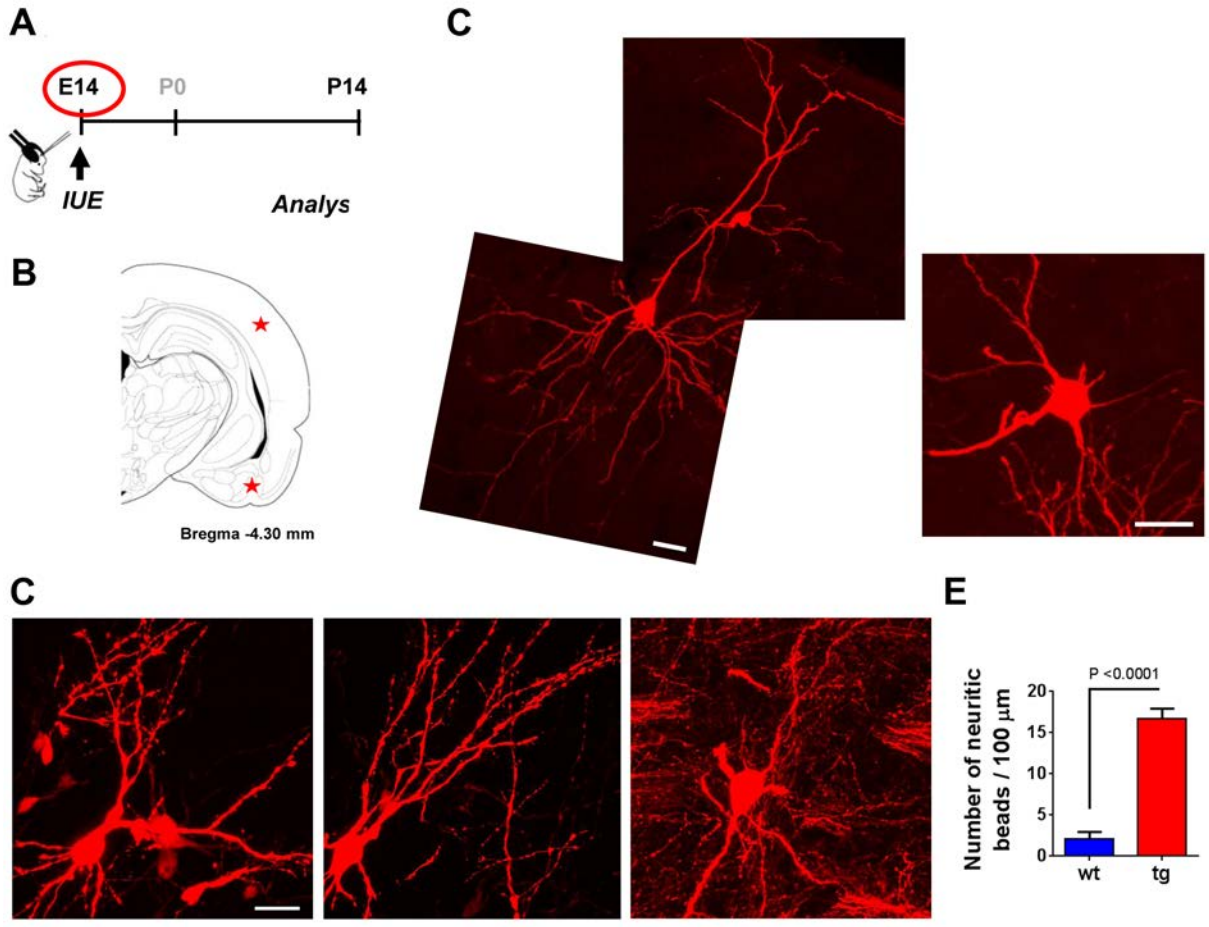

Fig. S3. Effect of HERV-K *env* in postnatal neurons of mice. (**A**) tdTomato with or without HERV-K *env* containing plasmid was introduced into the brain by intrauterine electroporation (IUE) on embryonic day 14 (E14). The animals were perfused and brains processed for immunohistochemistry on post natal day 14 (P14). (**B**) Coronal sections were made and cortical neurons were analyzed in regions shown with a star. (**C**) Animals injected with tdTomato only

showed normal neuronal morphology with smooth processes. (**D**) Representative neurons from animals injected with tdTomato and HERV-K *env* are shown in three panels. The neurons show beading of the processes. Scale bars are 20 µm. (**E**) The number of neuritic beads per 100 µm was quantified.

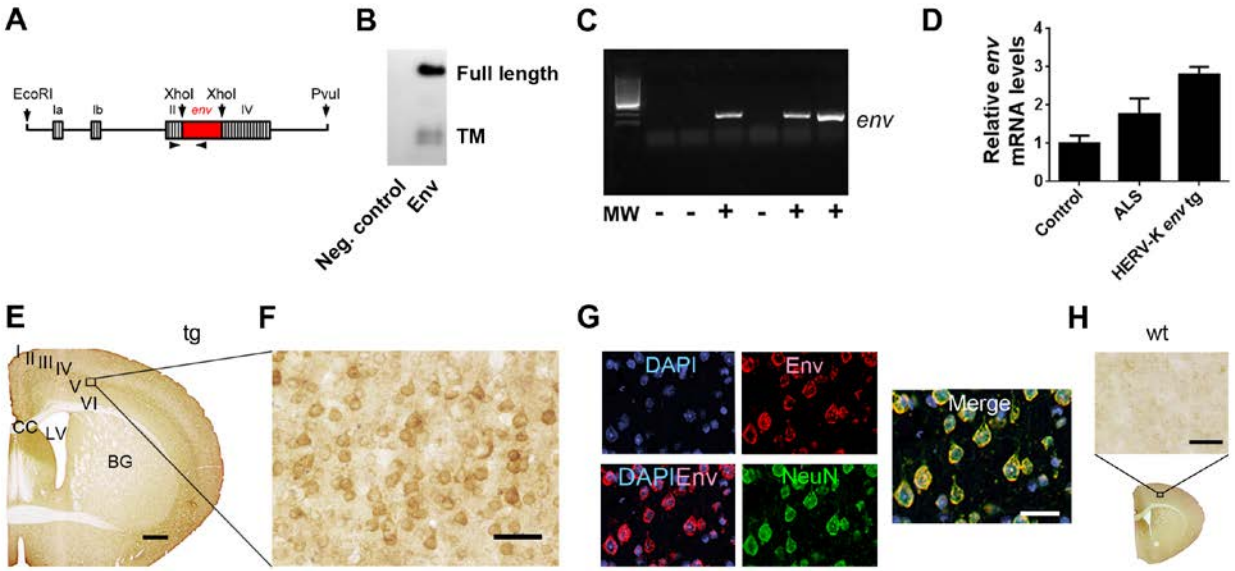

Fig. S4. Expression of HERV-K *env* in the brain of transgenic mice. (**A**) The diagram shows Thy1-*env* transgene construct used to generate tg mice. A 2.1kb fragment of the codon optimized HERV-K *env*, was subcloned into the XhoI site of the mouse Thy1.2 expression cassette. The untranslated exons of the Thy-1.2 gene are shown as striped bars. PCR primers for genotyping were chosen to span both the Thy1 region and the *env* region (indicated by arrows). (**B**) Total RNA was extracted from brain tissues of tg mice. Reverse transcription PCR was used to determine the expression of HERV-K *env* transgene mRNA. Genotype positive animals (+) showed a specific *env* PCR product, while genotype negative (-) animals had no amplification. (**C**) Levels of HERV-K *env* mRNA expression in patients with ALS and HERV-K *env* transgenic

mice were determined. As compared with healthy control human brain, the levels of expression were significantly high in both ALS patients and transgenic mice. GAPDH mRNA was used as an internal standard. (**D**) HeLa cells were transfected with either pcDNA3.1containing HERV-K *env* or empty vector (negative control). 48 hours post transfection, cells were harvested and cell lysate was subjected to Western blot analysis with HERV-K Env antibody. Only the cells with HERV-K *env* plasmid transfection showed specific immunoreactivity. The full length Env protein is 80kD, and transmembrane subunit is 42 kDa. (**E to G**) Brain tissues from 6-month old tg and their littermate wt mice were immunostaing with anti-HERV-K env antibody and then visualized using 3,3'-Diaminobenzidine (DAB) as a chromogen. (**E**) Strong env immunoreactivity was observed in the cerebral cortex. (**F**) A higher magnification of the area in the box in the left panel shows that env-positive cells have the morphology of cortical neurons with apical dendrites. (**G**) Env immunostaining in neurons was located primarily on the cell membrane and in the cytoplasm of the neuronal cell body. (**H**) The env-positive neurons were absent in wt brain. Scale bars are 500 μm (**E**) and 50 μm (**F** to **H**).

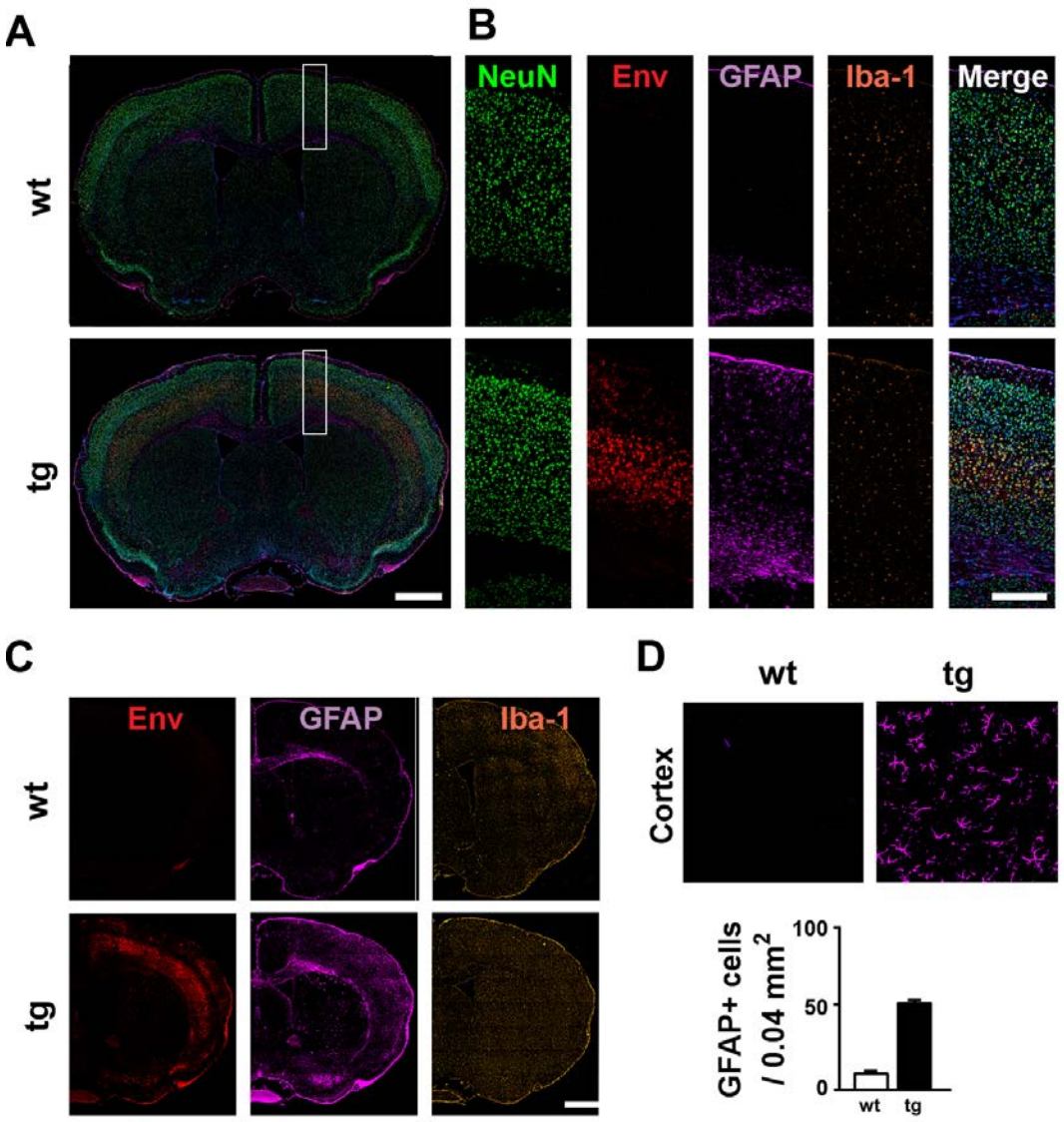

Fig. S5. Distribution of cellular proteins in wild type and HERV-K *env* transgenic mouse brains. (**A, B**) Coronal sections of wt and tg mouse brain at 6 months of age were immunostained for HERV-K env (red) and the following neuronal and glial markers: NeuN (green), a pan-neuronal marker; GFAP (purple), a marker for astrocytes; Iba-1 (orange), a marker for microglia. (**A**) Upper panel shows a whole brain section with merged images with each of the cellular markers and (**B**) enlarged images of cerebral cortex region (dashed boxed area in the left panel) showing individual cell types and HERV-K env expression. (**C**) The distribution of GFAP

(purple) and Iba-1 (orange) expression is shown in whole brain sections of wt and tg mice. (**D**) Sample images show GFAP immunoreactivity in the cortical cortex of wt and tg mice. For quantification, GFAP-positive cells were counted in at least three 200×200 μm fields from the cortical cortex for each animal evaluated. HERV-K *env* tg mice had significantly increased numbers of GFAP-positive cells in the cortex. Values represent mean ± SEM from three animals in each group and were analyzed by Student's *t* test. Scale bars are 2 mm (**A**), 500 μm (**B**), 2 mm (**C**), and 100 μm (**D**).

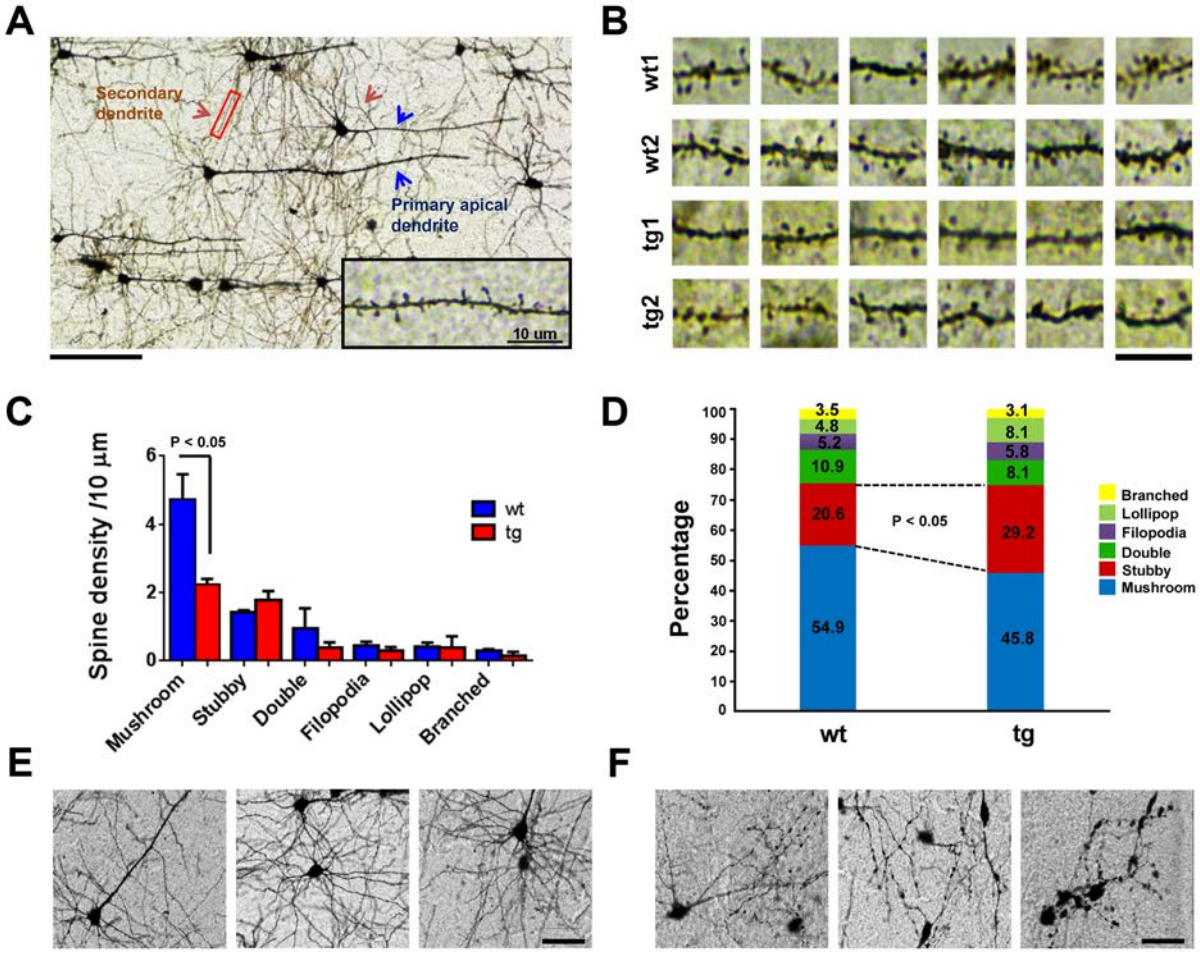

Fig. S6. Changes in spine morphology and dendritic damage in pyramidal neurons in HERV-K *env* transgenic mice. (**A**) Pyramidal neurons were captured for a segment 10 μm in

length of a secondary dendrite that ended in a fine taper to analyze dendritic spine. To be consistent in analysis of spine areas, the segment of dendrites located 10-30 μm from the tip of each dendritic branch was chosen. 30 dendrites were identified from each mouse brain. Insert shows a secondary dendrite under higher magnification. (**B**) Represenative micrographs show 10 □m ofdendritic spines of wt and tg mice used for analyzing. (**C**) The protrusion of dendritic spines was categorized into 6 types based on their shapes and lengths: mushroom, stubby, double, filopodia, llipop and branched spines. The density of mushroom spines decreased in the cortical neurons of tg mice. (**D**) Distribution of different types of dendritic protrusions was altered in tg mice. Values represent mean ± SEM from three animals in each group and were analyzed by Student's *t* test. (**E, F**) Disconnected dendritic beads and swellings are hallmarks of dendritic injury. (**E**) The dendrites in the wt mice were smooth with very few beadings. (**F**) Lots of dendritic beadings were seen in cortical neurons in the cortex of tg mice. Scale bars are 100 μm (**A**), 10 μm (**B**), and 50 μm (**E, F**).

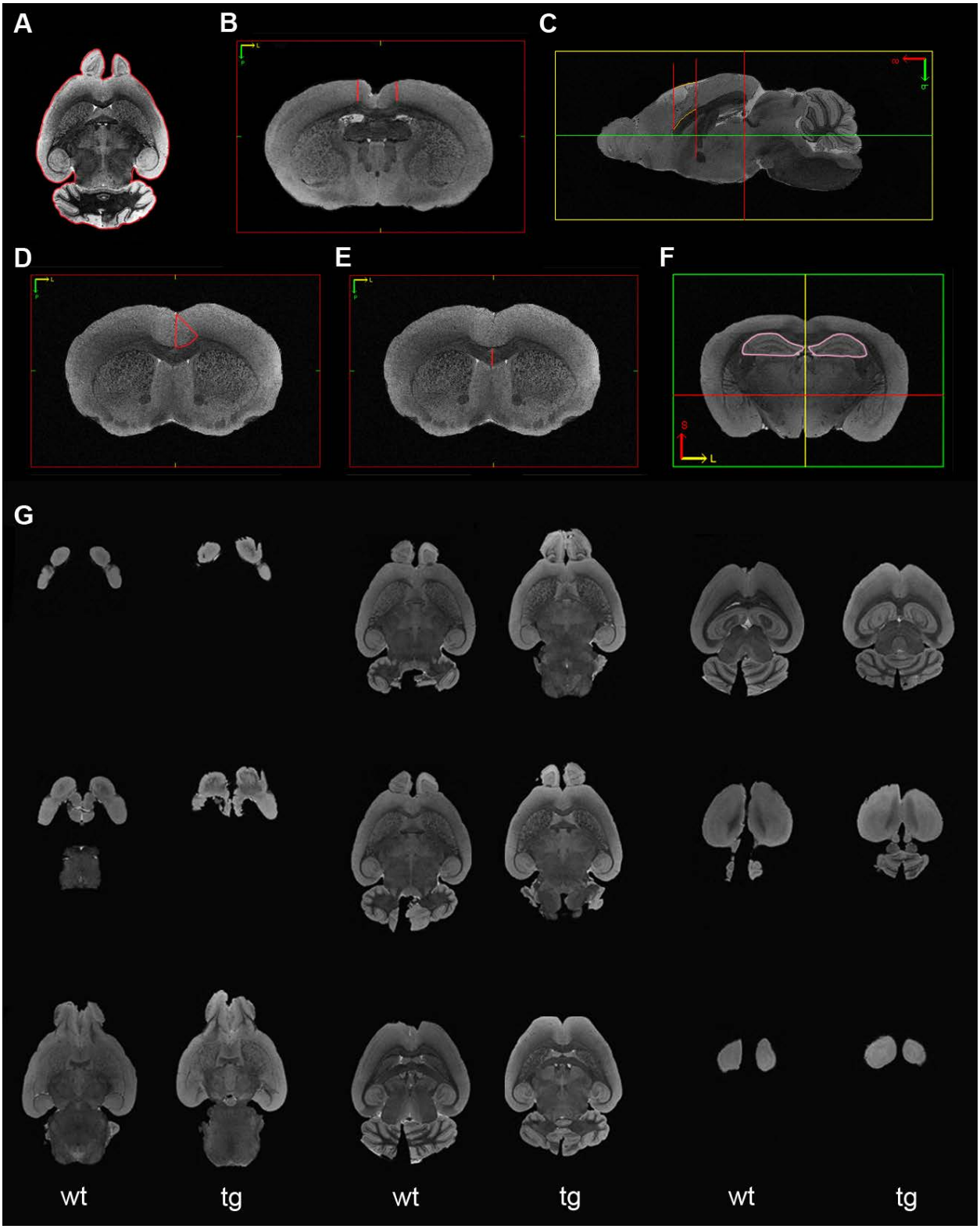
A
B
C
D
E
F
G
wt
tg
wt
tg
wt
tg

Fig. S7. MR imaging and regional analysis of mouse brains. 8 months old wild type and transgenic mice were subjected to MR imaging. (**A**) MRI sections showing examples of the ROI drawings for the whole brain volume, (**B**) the motor cortex thickness, (**C**) the motor cortex volume, (**D**) the cingulate cortex, (**E**) the corpus callosum and (**F**) the hippocampus. (**G**) Upon visual examination, no obvious structural differences between wild type and HERV-K *env* transgenic mice were seen.

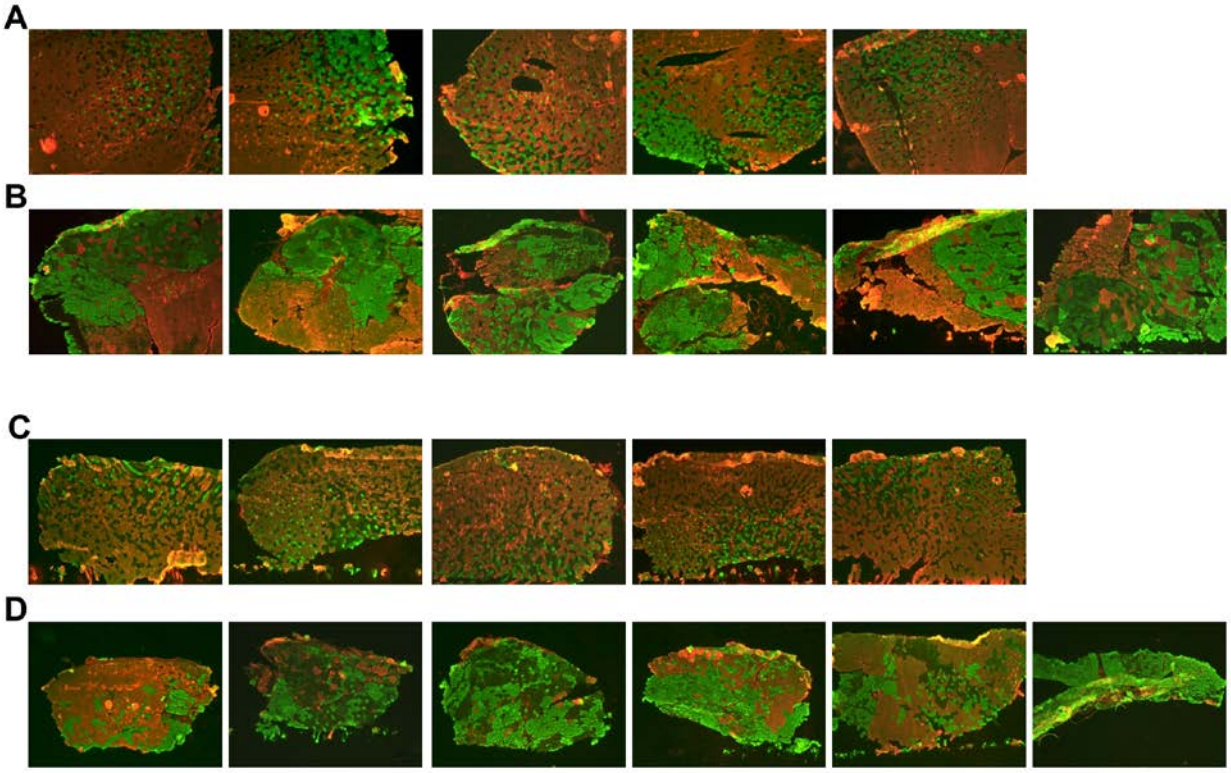

Fig. S8. Muscle pathology in HERV-K *env* transgenic mice. (A, B) Quadriceps and (**C,D**) tibialis anterior from wt and tg mice were isolated and processed for immunostaining with anti-MYH7 and anti-BF-F3. While the normal checkerbord patterns in (**A**) quadriceps muscle and (**C**) tibialis anterior of wt mice were seen, fiber type grouping and atrophy was found in (**B**) quadriceps muscle (**D**) and tibialis anterior of tg mice.

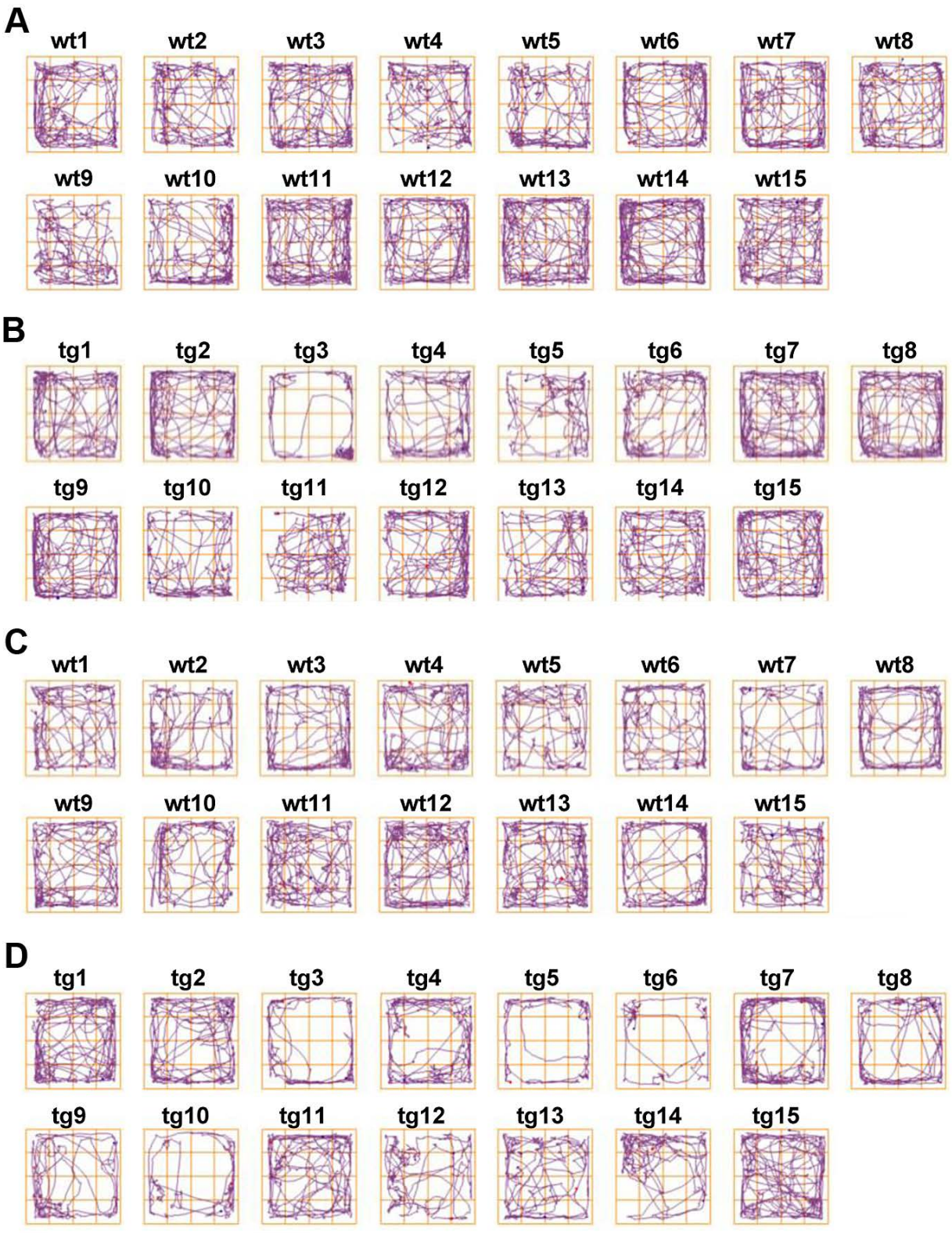
A
wt1
wt2
wt3
wt4
wt5
wt6
wt7
wt8
wt9
wt10
wt11
wt12
wt13
wt14
wt15
B
tg1
tg2
tg3
tg4
tg5
tg6
tg7
tg8
tg9
tg10
tg11
tg12
tg13
tg14
tg15
C
wt1
wt2
wt3
wt4
wt5
wt6
wt7
wt8
wt9
wt10
wt11
wt12
wt13
wt14
wt15
D
tg1
tg2
tg3
tg4
tg5
tg6
tg7
tg8
tg9
tg10
tg11
tg12
tg13
tg14
tg15

Fig. S9. Impairment of locomotor behavior in HERV-K *env* transgenic mice. **(A** to **D)** Spontaneous locomotion behavior was recorded during 5 min exploration in the open field. Compared to (**A**) age-matched wt littermates, (**B**) the 3 month-old tg mice entered the center less frequently. Similarly, compared to (**C**) wt littermates, (**D**) the 6 month-old tg mice spent much less time in the center of the open field.

A **TDP-43 binding sites on HERV-K LTR**

Oligonucleotide Name	Sequence (5' → 3')
Nt343#	5'-BIO-CAAGGTTTCTCCCCATGTGA-3'
Nt726#	5'–BIO-TGCTGACCCTCTCCCACAAT-3'
Nt761#	5'-BIO-ACACATCCCCCTCTTTGAGA-3'
Nt866#	5' –BIO-CCTTATTTCTTTCTCTATAC-3'
Nt893#	5' –BIO-GTGTCTTTTTCTTTTCCAAA-3'
Control	5'-BIO-CGGATATGATATCTATACCG-3'

Nt, nucleotide; BIO, biotin
# indicates position of the first base in the pyrimidine-rich sequence on HERV-K LTR (1-968bp)
Putative TDP-43 binding sites are underlined

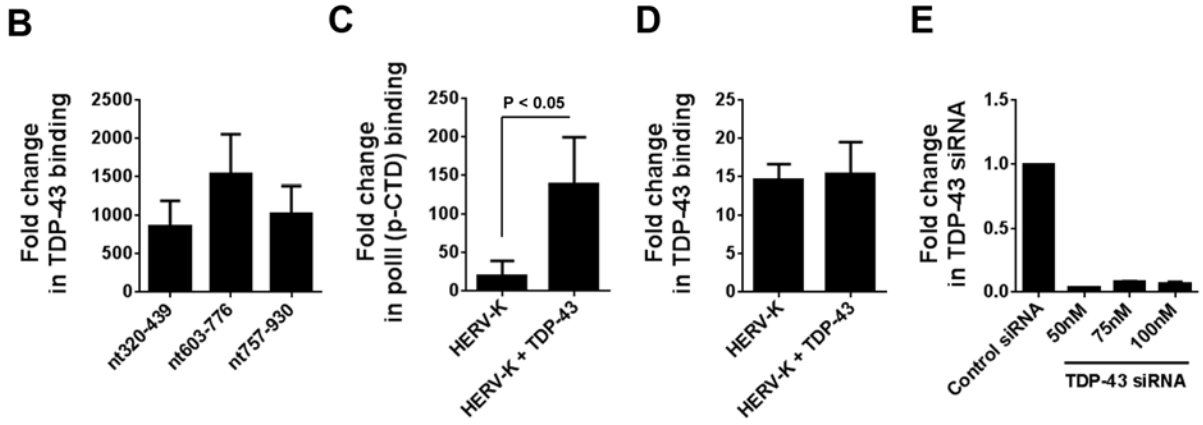

Fig. S10. TDP-43 binds to the HERV-K LTR in vivo, and TDP-43 binding to HERV-K LTR correlates with association of a processive RNA polymerase II (p-Ser2) on the LTR. (**A**) Putative TDP-43 binding sites (pyrimidine-rich regions) were identified on the HERV-K LTR. (**B**) TDP-43 associates with the HERV-K LTR. Hela cells were transiently transfected with

HERV-K LTR-luciferase construct and TDP-43 expression plasmid. 48 hours post-transfection, chromatin immunoprecipitation (ChIP) was performed using IgG control or antibody specific for TDP-43, followed by real-time PCR to amplify the indicated regions of the HERV-K LTR. (**C**) TDP-43 binding to HERV-K LTR is associated with increased binding of elongation-competent RNA polymerase II. HeLa cells were transfected with HERV-K LTR-luciferase construct with either vector control (pcDNA3.1) or TDP-43 expression plasmid. 48 hours post-transfection, cells were subjected to chromatin immunoprecipitation using antibody against the C-terminally phosphorylated form of RNA polymerase II (p-Ser2). Real time-PCR was performed to detect binding of RNA pol II on the HERV-K LTR. (**D**) Chromatin immunoprecipitation was performed as described in Materials and Methods using antibody specific for TDP-43 and real-time PCR was performed to detect binding at an unrelated genomic region (GAPDH promoter). No association was detected, indicating that the results in (**B**) and (**C**) are not due to DNA contamination or non-specific immunoprecipitation. (**E**) RT-PCR results showing efficacy of TDP-43 knockdown at 24 hours post-transfection with control or TDP-43 siRNA at 50-100 nM concentration. Values represent mean ± SD from at least three independent experiments and were analyzed by Student's *t* test.

SUPPLEMENTARY TABLES

Table S1. Clinical data for the human brain samples.

Subject #	Underlying illness	Cause of death	Age at death (yrs)	Gender	Race	PMI (hrs)	RNA sec
206	none	Rupture of aorta	76	M	unknown	unknown	
1573	none	Pedestrian hit by car	32	F	W	12	
1577	none	Asthma	34	F	B	12	
4637	none	Motor vehicle accident	31	F	W	17	
4676	none	Pedestrian hit by car	40	F	B	15	*
5030	none	Asthma	24	M	B	14	
5125	Asthma	Motor vehicle accident	24	F	W	9	
5189	none	Arrhythmia, drowning	40	M	W	14	*
5342	none	Motorcycle accident	22	M	B	14	
5343	Depression, anxiety, GERD	Gastric perforation after surgery	48	F	W	13	*
5346	none	Blunt force	24	F	W	14	
R1106	none	Bladder cancer	79	M	W	1.75	
R1153	none	Pancreatic cancer	75	F	W	3.5	
R1161	unknown	Cardiac arrest	84	F	W	2.5	
R1216	none	Lung cancer	79	F	W	1.75	
R1217	none	Metastatic prostate cancer	78	M	W	1.17	

Patient #	Diagnosis	Age at onset (yrs)	Site of Onset	Duration (mths)	C9ORF72	Age at death (yrs)	Gender	Race	PMI (hrs)	
4	sALS	63	Bulbar	6	No	63	F	W	13	*
7	sALS	66	Bulbar	14	Yes	67	M	W	8	
10	sALS	67	LE & Bulbar	27	No	70	F	W	3	
15	sALS	62	Left leg	31	No	65	M	W	6	*
21	sALS	51	Left foot	27	No	53	F	W	3	
32	sALS	58	Both LE	18	No	59	M	W	7	*
53	sALS	51	Left UE	36	No	54	M	W	9	
55	sALS	57	Both LE	46	No	61	F	W	5	
59	sALS	55	Both LE	52	No	61	F	W	14	
64	FTD/ALS	63	Both UE	13	No	64	M	W	6	
70	sALS	54	Left leg	98	No	63	M	W	6	

F, female; M, male; W, white; B, black; LE, lower extremity; UE, upper extremity; PMI, post mortem interval; GERD, gastroesophageal reflux

Table S2. Passive and active membrane properties of mPFC L5 pyramidal neurons.
RMP, resting membrane potential; AHP, after hyperpolarization. Parameters of the first spike were measured during a current ramp 200pA/s.

Variables	wt	tg	*p* values
Number of neurons	15	17	
PASSIVE MEMBRANE PROPERTIES			
RMP (mV)	-68.7 ± 0.6	-65.4 ± 1.2	*ns*
Input resistance (MΩ)	140.2 ± 20.2	219.8± 27.7	*
ACTIVE MEMBRANE PROPERTIES			
Rheobase (pA)	71.3 ± 7.9	51.4 ± 8.9	*
Threshold (mV)	-43.3 ± 0.9	-42.8± 1.1	*ns*
Amplitude (mV)	82.5 ± 2.8	78.4± 2.1	*ns*
Rise time 10-90% (ms)	0.34 ± 0.02	0.36 ± 0.01	*ns*
Latency (ms)	456.3 ± 4 7.3	316.8 ± 41.2	*
Width (mV)	0.98 ± 0.05	0.98 ± 0.02	*ns*
AHP amplitude (mV)	-10.4 ± 0.5	-10.0± 0.6	*ns*

Table S3. Primer sequences

	Primer sequence (5' to 3')
HERV-K *env*	Forward: CTGAGGCAATTGCAGGAGTT Reverse: GCTGTCTCTTCGGAGCTGTT
HERV-K *pol*	Forward: TCACATGGAAACAGGCAAAA Reverse: AGGTACATGCGTGACATCCA
HERV-K *gag*	Forward: AGCAGGTCAGGTGCCTGTAACATT Reverse: TGGTGCCGTAGGATTAAGTCTCCT
HERV-E *env*[3]	Forward: CTGGTCCACGCACGGCCGAAGCATG Reverse: AAAAGGACGACTTAATAGAGCCAAT
HERV-R *env* [3]	Forward: GGGCCAATTATGCTTACCAA Reverse: ATGGGCTGATCTGGCTCTAA
HERV-P *env* [4]	Forward: CAAGATTGGGTCCCCTCAC Reverse: CCTATGGGGTCTTTCCCTC
GAPDH	Forward: TGCACCACCAACTGCTTAGC Reverse: GGCATGGACTGTGGTCATGAG
tg-HERV-K *env*	Forward: GTGTGCCTGTTTTGTCTGC Reverse: CACGATCTGGTCCCTTTTACTC
mGAPDH	Forward: AGGTCGGTGTGAACGGATTTG Reverse: GGGGTCGTTGATGGCAACA

Supplementary Video 1. Hind limb clasping in a tail suspension test. (**A, B**) Muscle strength and reflexes were evaluated using the tail suspension test in wt and tg mice at 6 months of age. When mice were suspended by the tail for 15 sec, (**A**) a wt mouse shows normal plantar reaction while (**B**) a tg mouse shows limb clasping reaction.

Supplementary References

1. Agoni, L., Guha, C. & Lenz, J. Detection of Human Endogenous Retrovirus K (HERV-K) Transcripts in Human Prostate Cancer Cell Lines. *Frontiers in oncology* **3**, 180 (2013).
2. Flockerzi, A., *et al.* Expression patterns of transcribed human endogenous retrovirus HERV-K(HML-2) loci in human tissues and the need for a HERV Transcriptome Project. *BMC genomics* **9**, 354 (2008).
3. Kowalczyk, M.J., *et al.* Expression of selected human endogenous retroviral sequences in skin and peripheral blood mononuclear cells in morphea. *Archives of medical science : AMS* **8**, 819-825 (2012).
4. Ahn, K. & Kim, H.S. Structural and quantitative expression analyses of HERV gene family in human tissues. *Molecules and cells* **28**, 99-103 (2009).